

First structurally characterized self-assembly of bipodal *N*-thiophosphorylated bis-thiourea with Co^{II}: magnetic properties and thermal decomposition†

Cite this: *Dalton Trans.*, 2013, **42**, 5532

Damir A. Safin,^{*a} Maria G. Babashkina,^a Antoine P. Railliet,^a Nikolay A. Tumanov,^a Koen Robeyns,^a Eamonn Devlin,^b Yiannis Sanakis,^b Yaroslav Filinchuk^a and Yann Garcia^{*a}

Reaction of piperazine with isothiocyanate (iPrO)₂P(S)NCS leads to *N*-thiophosphorylated bis-thiourea (iPrO)₂P(S)NHC(S)NC₄H₈NC(S)NHP(S)(OiPr)₂ (**H₂L**). Recrystallization of **H₂L** from DMSO leads to the formation of the new ligand (iPrO)₂P(S)NC₄H₈NP(S)(OiPr)₂ (**1**). Reaction of doubly deprotonated **L** with Co^{II} leads to the [Co₂L₂] complex. The thermal properties of [Co₂L₂] in an air atmosphere were studied by means of TGA with the observed final residue corresponding to [CoPS₃]₂. The crystal structure of [Co₂L₂] was elucidated by single crystal X-ray diffraction. Two metal cations are in a tetrahedral 1,5-*S*₂*S*'₂ environment formed by the C=S and P=S sulfur atoms. Investigation of the temperature dependence of the magnetic susceptibility is consistent with two effectively non-interacting Co^{II} *S* = 3/2 ions.

Received 24th January 2013,

Accepted 31st January 2013

DOI: 10.1039/c3dt50254f

www.rsc.org/dalton

Introduction

In the literature there are only sixteen structurally characterized cobalt complexes with each having the imidodiphosphinate ligands R₂P(X)NP(Y)R'₂ (IDP)¹ and acylthioamides RC(X)NC(Y)R' (AA) or aroylthioureas R₂NC(X)NC(Y)R' (ATU)² (X, Y = O, S, Se). This might be explained by the structural versatility of the formed complexes (tetrahedral and octahedral) together with the oxidation state of the cobalt cation (Co^{II} and Co^{III}). Furthermore, there is only one structure of a Co^{II} complex with the bipodal ATU (X = S, Y = O) ligand, where two metal cations are coordinated by the deprotonated chelate backbones of two parent ligands through the sulfur and oxygen atoms and the oxygen atom of the methanol molecule, exhibiting a distorted pyramidal coordination core.^{2h}

The synthesis and complexation properties of *N*-(thio)phosphorylated thioamides and thioureas RC(S)NHP(X)(OR')₂ (X = O, S) (NTT), which are IDP's, AA's and ATU's asymmetrical analogues, have been extensively studied,³ but there is still limited information about structures of cobalt complexes with NTT. There are only eleven structures of Co^{II} complexes with

the deprotonated NTT ligands reported.⁴ No structurally characterized complexes of bipodal NTT with Co^{II} have been described so far.

In this work, we describe a complete structural investigation together with thermal and magnetic properties of the self-assembly of bipodal *N*-thiophosphorylated bis-thiourea (iPrO)₂P(S)NHC(S)NC₄H₈NC(S)NHP(S)(OiPr)₂ (**H₂L**) with Co^{II}.

Results and discussion

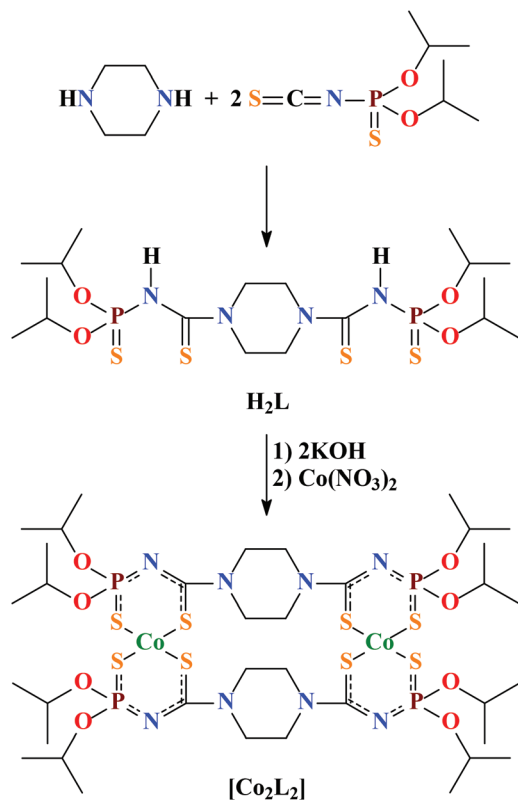
The ligand **H₂L** was prepared by reacting piperazine with the isothiocyanate (iPrO)₂P(S)NCS (Scheme 1). The obtained white powder is exclusively soluble in DMSO. The complex [Co₂L₂] was prepared by the following procedure: the ligand was deprotonated *in situ* using KOH, followed by the reaction with Co(NO₃)₂·6H₂O (Scheme 1). The obtained green material is soluble in all common solvents except diethyl ether, *n*-hexane and water.

The IR spectrum of [Co₂L₂] contains a band at 605 cm⁻¹ for the P=S group of the anionic forms **L**, which is 37 cm⁻¹ shifted to low frequencies compared to that in the spectrum of the parent ligand **H₂L**. In the spectrum of the complex there is an intense band at 1546 cm⁻¹, corresponding to the conjugated SCN fragment. The IR spectrum of **H₂L** also contains the characteristic band for the NH groups at 3314 cm⁻¹, while no band for the NH group was observed in the spectrum of [Co₂L₂]. In addition, there is a broad intense band arising from the POC group at 998–1004 cm⁻¹ in the spectra of the ligand and the complex.

^aInstitute of Condensed Matter and Nanosciences, MOST – Inorganic Chemistry, Université Catholique de Louvain, Place L. Pasteur 1, 1348 Louvain-la-Neuve, Belgium. E-mail: damir.safin@ksu.ru, yann.garcia@uclouvain.be; Fax: +32 (0) 1047 2330; Tel: +32 (0) 1047 2831

^bInstitute of Materials Science, NCSR Demokritos, Athens 15310, Greece

† Electronic supplementary information (ESI) available: Fig. S1–S3, Tables S1–S4. CCDC 911407–911409. For ESI and crystallographic data in CIF or other electronic format see DOI: 10.1039/c3dt50254f

Scheme 1 Preparation of H_2L and $[\text{Co}_2\text{L}_2]$.

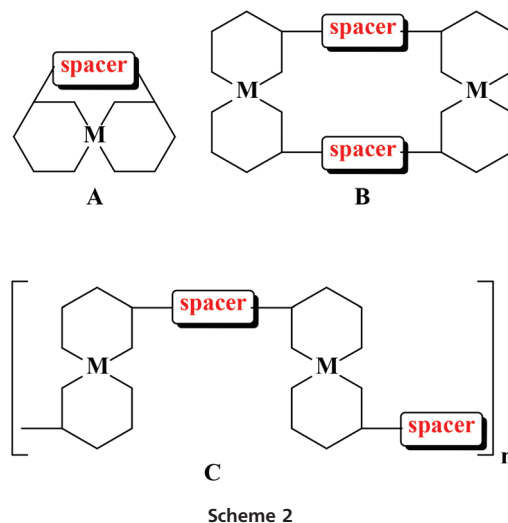
$^{31}\text{P}\{^1\text{H}\}$ and ^1H NMR spectroscopy data allow us to establish the structure of the ligand H_2L and to confirm the fact of reaction of isothiocyanate with both NH groups of piperazine. There is a singlet at 62.8 ppm in the $^{31}\text{P}\{^1\text{H}\}$ NMR spectrum of H_2L . The signal is in the region that is characteristic for NTT ($X = \text{S}$).³ The ^1H NMR spectrum of H_2L contains a set of signals assigned to the *iPr* protons: a doublet at 1.19 ppm and a doublet of septets at 4.66 ppm. The signals of the CH_2 protons, corresponding to the piperazine fragment, are 2.47 and 2.73 ppm. A broad singlet at 8.14 ppm derives from the PNH protons.

No NMR spectra of $[\text{Co}_2\text{L}_2]$ were obtained due to the paramagnetic character of the $d^7 \text{Co}^{\text{II}}$.

According to elemental analysis, the complex $[\text{Co}_2\text{L}_2]$ has a ratio of $\text{M}:\text{L} = 1:1$. Divalent metals can form complexes of 1:1 $[\text{ML}]$ (A) and 2:2 $[\text{M}_2\text{L}_2]$ (B) compositions with such bipodal ligands. A formation of oligomeric or polymeric composition $[\text{M}_n\text{L}_n]$ (C) is also possible (Scheme 2).

We assume that the structure of complexes depends first of all on the length and rigidity of bridging chains between two chelate moieties and secondly on the nature of metal cations. Earlier it has been shown that for complexes of the bifunctional NTT ligands dimeric molecules are formed in a growing crystal (Scheme 2, B).⁵

The structure of the chelate unit in $[\text{Co}_2\text{L}_2]$ in a CH_2Cl_2 solution was established by UV-vis spectroscopy. The spectrum is characterized by three intense bands in the UV region at 257



Scheme 2

($\epsilon = 71\,850 \text{ M}^{-1} \text{ cm}^{-1}$), 308 ($\epsilon = 34\,385 \text{ M}^{-1} \text{ cm}^{-1}$) and 379 ($\epsilon = 24\,060 \text{ M}^{-1} \text{ cm}^{-1}$) nm, which are attributed to intraligand transitions. In the visible range, there is a structured absorption band with maxima at 554 ($\epsilon = 517 \text{ M}^{-1} \text{ cm}^{-1}$), 613 ($\epsilon = 562 \text{ M}^{-1} \text{ cm}^{-1}$) and 665 ($\epsilon = 342 \text{ M}^{-1} \text{ cm}^{-1}$) nm. This absorption band corresponds to a transition from the ground state $^4\text{A}_2$ to a $^4\text{T}_1(\text{P})$ state. The fine-structure (several maxima) is caused by the spin-orbital interaction as a result of which, first, there is a splitting of the state $^4\text{T}_1(\text{P})$ and, secondly, there are resolved transitions in the next doublet states with the same intensity. The other possible transitions $^4\text{A}_2 \rightarrow ^4\text{T}_2$ and $^4\text{A}_2 \rightarrow ^4\text{T}_1(\text{F})$ are expected beyond the visible area with poor intensities. Thus, UV-vis spectroscopy unequivocally confirms the tetrahedral environment of the Co^{II} cations in $[\text{Co}_2\text{L}_2]$ at least in CH_2Cl_2 . It is necessary to note that the values of ϵ are approximately twice larger than for the mononuclear Co^{II} complexes with NTT.⁴ This fact testifies the formation of the complex of the 2:2 $[\text{M}_2\text{L}_2]$ composition at least in CH_2Cl_2 (Scheme 2, B).

The compounds H_2L and $[\text{Co}_2\text{L}_2]$ were also analysed by diffuse reflectance spectroscopy as pure solid powders to avoid matrix and environment effects. The diffuse reflectance spectrum of H_2L contains a number of bands exclusively in the UV region, which are attributed to intraligand transitions (Fig. 1). The diffuse reflectance spectrum of $[\text{Co}_2\text{L}_2]$ exhibits two regions: three bands in the UV region, corresponding to the intraligand transitions of the deprotonated ligands L, and a second range from about 500 to 1100 nm (Fig. 1). The latter bands originate from the same transitions observed in the UV-vis spectrum of $[\text{CoL}_2]$ in CH_2Cl_2 (see above). However, diffuse reflectance spectroscopy has allowed us to observe the band at 800–1100 nm (Fig. 1). Thus, diffuse reflectance spectroscopy testifies the tetrahedral environment of the Co^{II} cation in $[\text{Co}_2\text{L}_2]$ in the solid state.

The thermal properties of H_2L and $[\text{Co}_2\text{L}_2]$ in an air atmosphere were studied by means of TGA to determine their respective stabilities (Fig. 2). Both compounds are stable up to about 100 °C and decomposed in four clearly defined steps

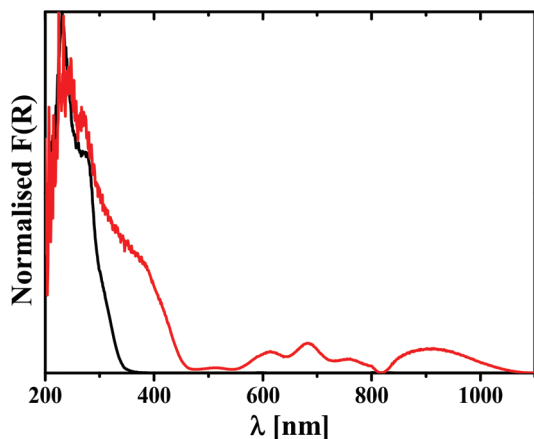


Fig. 1 Normalised Kubelka–Munk spectra of H_2L (black) and $[\text{Co}_2\text{L}_2]$ (red) at 298 K.

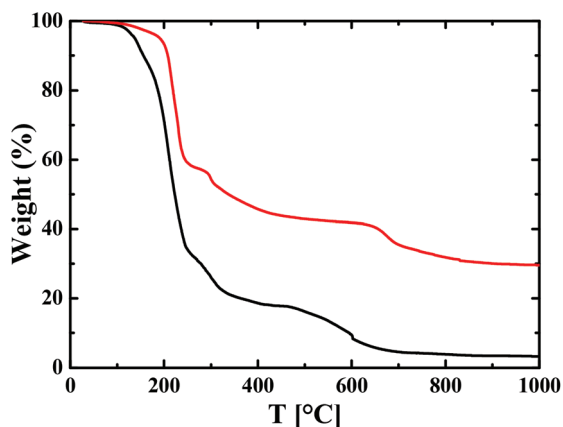


Fig. 2 TGA of H_2L (black) and $[\text{Co}_2\text{L}_2]$ (red) performed in a dynamic air atmosphere.

(Fig. 2). The observed final residue for $[\text{Co}_2\text{L}_2]$ is 29.3 wt%. This value is in excellent agreement with the calculated 29.6 wt% for $[\text{CoPS}_3]_2$, for which the commonly used synthesis from pure elements is quite complicated and requires specific conditions.⁶ The formation of $[\text{CoPS}_3]_2$ was proved based on elemental analysis data (calc.: S 51.69%, found: S 51.83%) and IR spectroscopy, where the majority of the features correspond to vibrational transitions, which have been discussed previously, and the band positions agree closely with those reported previously for P–S and Co–S deformations (Fig. S1 in ESI[†]).⁷ There is also a full correspondence with recorded and calculated PXRD data from a single crystal analysis (JCPDS 42-0824) (Fig. S2 in ESI[†]).⁶

Numerous attempts to obtain X-ray suitable crystals of the parent ligand H_2L by recrystallization from DMSO have failed. Instead, the unprecedented formation of colourless single crystals of the *N*-thiophosphorylated piperazine (**1**) was observed with almost a quantitative yield. The IR spectrum of **1** contains bands for the P=S and POC groups at 636 and 1014 cm^{-1} , respectively. The $^{31}\text{P}\{^1\text{H}\}$ spectrum contains a singlet signal at

65.6 ppm. The ^1H NMR spectrum of **1** shows a set of signals assigned to the *i*Pr protons: a doublet at 1.28 ppm and a doublet of septets at 4.49 ppm. The signals of the CH_2 protons, corresponding to the piperazine fragment, are 2.25 and 2.32 ppm. According to X-ray data, **1** crystallizes in the monoclinic space group $C2/c$. Results of the structure solution and refinements are collected in ESI[†]. Bonding parameters are listed in Table S1 in ESI[†]. The molecular structure is shown in Fig. 3. The $(\text{iPrO})_2\text{P}=\text{S}$ groups in the structure of **1** were found in a *trans*-configuration (Fig. 3). The P=S and P–N bond lengths are 1.9228(6) and 1.6521(14) Å, respectively, with the S–P–N angle being 114.27(5)° (Table S1 in ESI[†]). Compound **1** is an intriguing synthon for coordination chemistry. Complexation properties of **1** are currently under investigation and will be reported elsewhere.

Crystals of $[\text{Co}_2\text{L}_2]$ were obtained by slow evaporation of a saturated solution in ethyl acetate–*n*-hexane (1 : 5, v/v). Surprisingly, colourless crystals of piperazinium diacetate (**2**) were also formed due to partial hydrolysis of the complex. Results of the structure solution and refinements of $[\text{Co}_2\text{L}_2]$ and **2** are collected in ESI[†]. Geometric parameters are listed in Tables S2 and S3 in ESI[†]. The molecular structures are shown in Fig. 4 and 5, respectively.

According to X-ray data, $[\text{Co}_2\text{L}_2]$ crystallizes in the triclinic space group $P\bar{1}$. Two doubly deprotonated ligands **L** are coordinated to two Co^{II} cations through the sulfur atoms of the C=S and P=S groups with the formation of two spirocyclic chelate

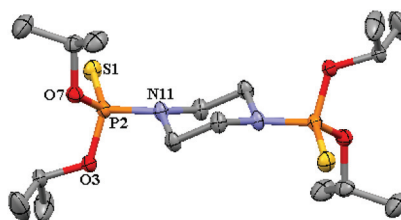


Fig. 3 Thermal ellipsoid (50%) plot of **1**. H-atoms were omitted for clarity.

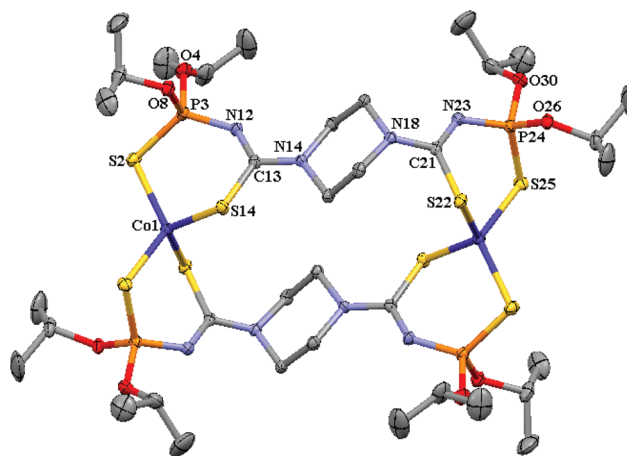


Fig. 4 Thermal ellipsoid (50%) plot of $[\text{Co}_2\text{L}_2]$. H-atoms were omitted for clarity.

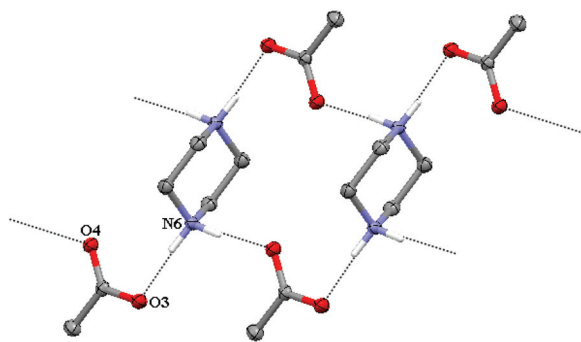


Fig. 5 Thermal ellipsoid (50%) plot of **2**. H-atoms, not involved in hydrogen bonding, were omitted for clarity.

backbones with distorted tetrahedral CoS_4 cores (Fig. 4). The Co–S(P) bond lengths are about 0.03–0.05 Å longer than the Co–S(C) bonds (Table S2 in ESI†). Notably, one of the Co–S(P) bond lengths is about 0.015 Å longer than the other, while the Co–S(C) bonds are very similar (Table S2 in ESI†). As expected the C–S, P–S and C–N(P) are somewhat elongated, while the P–N bonds are shortened compared to those of deprotonated **NTT** (X = S) (Table S2 in ESI†).³ The endocyclic angles S–Co–S_{endo} are reduced and the exocyclic angles S–Co–S_{exo} are increased in comparison with the ideal tetrahedral angle of 109.5° (Table S2 in ESI†). The six membered CoSPNCs cycles have the conformation of a distorted boat with planar PNCS fragments.

In the crystal structure of the salt **2** both NH groups of the piperazine fragment were found to be protonated with the formation of quaternary nitrogen atoms (Fig. 5, Table S3 in ESI†). Each of two acetate anions are bonded to the piperazinium dication through the hydrogen bond formed between one of the oxygen atoms of the anion and one of the NH hydrogen atoms of the cation (Fig. 5, Table S4 in ESI†). The second oxygen atom of the acetate anion forms a hydrogen bond with one of the NH protons of the neighbouring piperazinium dication resulting in the formation of a 1D polymeric chain (Fig. 5, Table S4 in ESI†).

Variable temperature magnetic susceptibility measurements of a crystalline sample of $[\text{Co}_2\text{L}_2]$ were carried out in the temperature range 5–300 K (Fig. 6). At 300 K, the $\chi_M T$ product is 4.59 $\text{cm}^3 \text{mol}^{-1} \text{K}$ which is of the order of magnitude expected for two spins with $S = 3/2$ and a Landé factor $g > 2.0$.⁸ As the temperature is lowered, $\chi_M T$ exhibits a smooth linear decrease down to ~70 K. Below this temperature the decrease is more abrupt reaching a value of 2.83 $\text{cm}^3 \text{mol}^{-1} \text{K}$ at 5 K. Simulations of the data using a Heisenberg spin Hamiltonian indicated that any exchange interaction should be relatively weak $|J| < 0.1 \text{ cm}^{-1}$. An inspection of the crystal structure (Fig. 4) indicates that the Co^{II} ions exhibit an intra-molecular distance of 8.8 Å whereas inter-molecular Co...Co separations are ~10 Å. These distances suggest weak magnetic interactions; to a first approximation the system can be considered as two isolated $S = 3/2$ spins obeying the zero field splitting

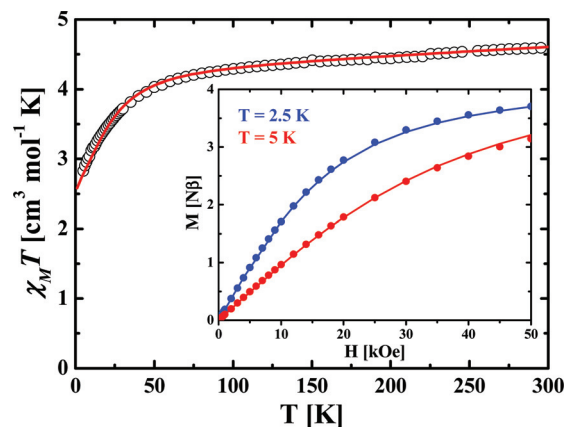


Fig. 6 Temperature dependence of $\chi_M T$ from a powder sample of $[\text{Co}_2\text{L}_2]$ in the presence of an external field of 0.1 T. The inset shows the field dependence of magnetization at 2.5 and 5 K. Solid lines are theoretical simulations as described in the text.

(ZFS) spin Hamiltonian:

$$\hat{H}_{\text{ZFS}} = D \left[S_z^2 - \frac{5}{4} \right] + E [S_x^2 - S_y^2] + \beta \bar{S} \vec{g} \vec{H}$$

The abrupt drop of $\chi_M T$ below 70 K is presumably due to the effect of ZFS, whereas the linear dependence of $\chi_M T$ above 70 K may be ascribed to the contribution of the Temperature Independent Paramagnetism (TIP). Satisfactory simulations of the temperature dependence of $\chi_M T$ were obtained using ZFS parameter $|D| = 24.8 \text{ cm}^{-1}$, $g = 2.12$ and TIP = $12.55 \times 10^{-4} \text{ cm}^3 \text{mol}^{-1}$. This model is further supported by magnetization data recorded as a function of the applied magnetic field at 2.5 K and 5 K (inset of Fig. 6). The magnetization data at both temperatures were reproduced with the same set of parameters with an E/D ratio of 0.33. These values are consistent with other tetra-coordinated Co^{II} complexes.⁹

Conclusions

In summary, we have synthesized the binuclear homoleptic Co^{II} complex with *N*-thiophosphorylated bis-thiourea (iPrO)₂-P(S)NHC(S)NC₄H₈NC(S)NHP(S)(OiPr)₂ (**H₂L**). It was established that both in the solid state and in solution the complex maintains its nuclearity and exhibits tetrahedral complex cores with the 1,5- $S_2S'_2$ environment of a metal center formed by the C=S and P=S sulfur atoms.

The thermal decomposition of $[\text{Co}_2\text{L}_2]$ in an air atmosphere resulted in the formation of the final residue, corresponding to $[\text{CoPS}_3]_2$.

Recrystallization of **H₂L** in DMSO leads to the unprecedented formation of the *N*-thiophosphorylated piperazine (**1**), which is an intriguing precursor for coordination chemistry. Furthermore, an attempt to obtain X-ray suitable crystals of $[\text{Co}_2\text{L}_2]$ from a mixture of ethyl acetate-*n*-hexane leads to

partial hydrolysis of the complex with the formation of piperazinium diacetate (2).

The magnetic susceptibility data of $[\text{Co}_2\text{L}_2]$ were well reproduced assuming two isolated Co^{II} ($S = 3/2$) ions with negligible magnetic interactions which are justified by the relatively large intramolecular $\text{Co}\cdots\text{Co}$ distance imposed by the long bridging ligand L.

Experimental

General procedures

Elemental analyses were performed on a Thermoquest Flash EA 1112 Analyzer from CE Instruments. The infrared spectrum (KBr) was recorded with a FTIR-8400S SHIMADZU spectrophotometer in the range $400\text{--}3600\text{ cm}^{-1}$. NMR spectra (DMSO-d_6) were obtained on a Bruker Avance 300 MHz spectrometer at $25\text{ }^\circ\text{C}$. ^1H and $^{31}\text{P}\{^1\text{H}\}$ NMR spectra were recorded at 299.948 and 121.420 MHz, respectively. Chemical shifts are reported with reference to SiMe_4 (^1H) and 85% H_3PO_4 ($^{31}\text{P}\{^1\text{H}\}$). The UV-vis absorption spectrum of a 10^{-4} M solution in CH_2Cl_2 was recorded on a Lambda-35 spectrometer in the range $200\text{--}1000\text{ nm}$. Diffuse reflectance spectra were obtained with a Varian Cary 5E spectrometer using polytetrafluoroethylene (PTFE) as a reference. Thermogravimetric (TGA) analyses were performed by a SDT 2960 Simultaneous DTA-TGA instrument in a dynamic air atmosphere (100 mL min^{-1}) from laboratory temperature to $1000\text{ }^\circ\text{C}$ with a $10\text{ }^\circ\text{C min}^{-1}$ heating. Magnetic susceptibility measurements were performed on a MPMS-5500 Quantum Design instrument in the temperature range $5\text{--}300\text{ K}$. The M vs. T data were collected both in heating and cooling modes and the data are superimposable (Fig. S3 in ESI †). Magnetization vs. H measurements were carried out at liquid helium temperatures and no hysteresis was observed (Fig. S3 in ESI †). Additionally, magnetization vs. H measurements were recorded at 100 K and 295 K to confirm the absence of ferromagnetic impurities. Experimental data were corrected for the sample holder and for the diamagnetic contribution of the sample.

Synthesis of H_2L

A solution of piperazine (0.431 g, 5 mmol) in anhydrous CH_2Cl_2 (15 mL) was treated under vigorous stirring with a solution of $(\text{iPrO})_2\text{P}(\text{S})\text{NCS}$ (2.868 g, 12 mmol) in the same solvent (15 mL). The mixture was stirred for 1 h. The formed white powder was filtered. Yield 2.739 g (97%). IR, ν : 642 (P=S), 998 (POC), 3314 (NH) cm^{-1} . ^1H NMR, δ : 1.19 (d, $^3J_{\text{H,H}} = 6.1\text{ Hz}$, 24H, CH_3 , iPr), 2.47 (br. s, 4H, CH_2 , piperazine), 2.73 (br. s, 4H, CH_2 , piperazine), 4.66 (d. s, $^3J_{\text{H,H}} = 6.1\text{ Hz}$, $^3J_{\text{POCH}} = 9.7\text{ Hz}$, 4H, OCH, iPr), 8.14 (br. s, 2H, NH) ppm. $^{31}\text{P}\{^1\text{H}\}$ NMR, δ : 62.8 ppm. Anal. Calc. for $\text{C}_{18}\text{H}_{38}\text{N}_4\text{O}_4\text{P}_2\text{S}_4$ (564.71): C 38.28, H 6.78, N 9.92. Found: C 38.41, H 6.84, N 9.82%.

Synthesis of 1

H_2L (0.18 mmol, 0.1 g) was dissolved in DMSO (5 mL). Colorless crystals were formed after slow evaporation of the solvent

for two days. Yield 0.075 g (93%). IR, ν : 636 (P=S), 1014 (POC) cm^{-1} . ^1H NMR, δ : 1.28 (d, $^3J_{\text{H,H}} = 6.0\text{ Hz}$, 24H, CH_3 , iPr), 2.25 (br. s, 4H, CH_2 , piperazine), 2.32 (br. s, 4H, CH_2 , piperazine), 4.49 (d. s, $^3J_{\text{H,H}} = 6.0\text{ Hz}$, $^3J_{\text{POCH}} = 10.7\text{ Hz}$, 4H, OCH, iPr) ppm. $^{31}\text{P}\{^1\text{H}\}$ NMR, δ : 65.6 ppm. Anal. Calc. for $\text{C}_{16}\text{H}_{36}\text{N}_2\text{O}_4\text{P}_2\text{S}_2$ (446.54): C 43.04, H 8.13, N 6.27. Found: C 43.11, H 8.19, N 6.21%.

Synthesis of $[\text{Co}_2\text{L}_2]$

A suspension of H_2L (0.565 g, 1 mmol) in MeOH (10 mL) was mixed with a MeOH solution of KOH (0.124 g, 2.2 mmol). A MeOH (10 mL) solution of $\text{Co}(\text{NO}_3)_2\cdot 6\text{H}_2\text{O}$ (0.350 g, 1.2 mmol) was added dropwise under vigorous stirring to the resulting potassium salt. The mixture was stirred at room temperature for a further 3 h and left overnight. The resulting complex was extracted with CH_2Cl_2 , washed with water and dried with anhydrous CaCl_2 . The solvent was then removed *in vacuo*. Green crystals were isolated by recrystallisation from a 1 : 3 mixture of CH_2Cl_2 and *n*-hexane. Yield 0.541 g (87%). IR, ν : 605 (P=S), 1004 (POC), 1546 (SCN) cm^{-1} . UV-vis, λ_{max} (ϵ , $\text{M}^{-1}\text{ cm}^{-1}$): 257 (71 850), 308 (34 385), 379 (24 060), 554 (517), 613 (562) and 665 (342) nm. Anal. Calc. for $\text{C}_{36}\text{H}_{72}\text{Co}_2\text{N}_8\text{O}_8\text{P}_4\text{S}_8$ (1243.26): C 34.78, H 5.84, N 9.01. Found: C 34.62, H 5.88, N 8.95%.

X-ray crystallography

X-ray data collection was performed on a Mar345 image plate detector using Mo-K α radiation (rotation anode, multilayer mirror) at $150(2)\text{ K}$ for 1 and 2 and at $296(2)\text{ K}$ for $[\text{Co}_2\text{L}_2]$. The data were integrated with the CrysAlisPro software.¹⁰ The implemented empirical absorption correction was applied. The structures were solved by direct methods using the SHELXS-97 program¹¹ and refined by full-matrix least squares on $|F^2|$ using SHELXL-97.¹¹ Non-hydrogen atoms were anisotropically refined and the hydrogen atoms were placed on calculated positions in riding mode with temperature factors fixed at 1.2 times U_{eq} of the parent atoms and 1.5 times U_{eq} for methyl groups. Figures were generated using the program Mercury.¹²

Crystal data for 1. $\text{C}_{16}\text{H}_{36}\text{N}_2\text{O}_4\text{P}_2\text{S}_2$, $M_r = 446.53\text{ g mol}^{-1}$, monoclinic, space group $C2/c$, $a = 17.7793(5)$, $b = 7.9981(2)$, $c = 17.2729(6)$ Å, $\beta = 91.163(3)^\circ$, $V = 2455.71(13)$ Å³, $Z = 4$, $\rho = 1.208\text{ g cm}^{-3}$, $\mu(\text{Mo-K}\alpha) = 0.368\text{ mm}^{-1}$, reflections: 11 873 collected, 3286 unique, $R_{\text{int}} = 0.052$, $R_1(\text{all}) = 0.0410$, $wR_2(\text{all}) = 0.1117$.

Crystal data for $[\text{Co}_2\text{L}_2]$. $\text{C}_{36}\text{H}_{72}\text{Co}_2\text{N}_8\text{O}_8\text{P}_4\text{S}_8$, $M_r = 1243.24\text{ g mol}^{-1}$, triclinic, space group $P\bar{1}$, $a = 10.2715(14)$, $b = 10.7122(13)$, $c = 14.188(3)$ Å, $\alpha = 91.162(13)$, $\beta = 92.255(14)$, $\gamma = 101.349(11)^\circ$, $V = 1528.8(4)$ Å³, $Z = 1$, $\rho = 1.350\text{ g cm}^{-3}$, $\mu(\text{Mo-K}\alpha) = 0.9682\text{ mm}^{-1}$, reflections: 6947 collected, 3771 unique, $R_{\text{int}} = 0.073$, $R_1(\text{all}) = 0.0576$, $wR_2(\text{all}) = 0.1535$.

Crystal data for 2. $\text{C}_8\text{H}_{18}\text{N}_2\text{O}_4$, $M_r = 206.24\text{ g mol}^{-1}$, triclinic, space group $P\bar{1}$, $a = 5.7855(3)$, $b = 7.0039(11)$, $c = 7.4459(11)$ Å, $\alpha = 117.795(16)$, $\beta = 100.317(9)$, $\gamma = 90.118(9)^\circ$, $V = 261.32(7)$ Å³, $Z = 1$, $\rho = 1.311\text{ g cm}^{-3}$, $\mu(\text{Mo-K}\alpha) = 0.104\text{ mm}^{-1}$,

reflections: 913 collected, 913 unique, $R_{\text{int}} = 0.000$, $R_1(\text{all}) = 0.0448$, $wR_2(\text{all}) = 0.1096$.

Acknowledgements

This work was funded by the Fonds National de la Recherche Scientifique-FNRS (IISN 4.4507.10). We thank the F.R.S.-FNRS (Belgium) for a post-doctoral position allocated to D. A. Safin and WBI (Belgium) for post-doctoral positions allocated to D. A. Safin and M. G. Babashkina. We also acknowledge the Fonds Spéciaux de Recherche (UCL) for the incoming post-doctoral fellowship co-funded by the Marie Curie actions of the European Commission granted to N. A. Tumanov. We are grateful to the COST action MP1202. "Rational design of hybrid organic-inorganic interfaces: the next step towards advanced functional materials".

Notes and references

- (a) F. Benabicha, A. Courtois, J. J. Delpuech, E. Elkaim, J. Hubsch, L. Rodehuser and P. Rubini, *Polyhedron*, 1986, **5**, 2005; (b) C. Silvestru, R. Rosler, I. Haiduc, R. Cea-Olivares and G. Espinosa-Perez, *Inorg. Chem.*, 1995, **34**, 3352; (c) C. Silvestru, R. Rosler, J. E. Drake, J. Yang, G. Espinosa-Perez and I. Haiduc, *J. Chem. Soc., Dalton Trans.*, 1998, 73; (d) J. Novosad, M. Necas, J. Marek, P. Veltsistas, C. Papadimitriou, I. Haiduc, M. Watanabe and J. D. Woollins, *Inorg. Chim. Acta*, 1999, **290**, 256; (e) L. M. Gilby and B. Piggott, *Polyhedron*, 1999, **18**, 1077; (f) J. Ellermann, W. Bauer, M. Dotzler, F. W. Heinemann and M. Moll, *Monatsh. Chem.*, 1999, **130**, 1419; (g) M. C. Aragoni, M. Arca, A. Garau, F. Isaia, V. Lippolis, G. L. Abbati and A. C. Fabretti, *Z. Anorg. Allg. Chem.*, 2000, **626**, 1454; (h) P. Sekar and J. A. Ibers, *Inorg. Chim. Acta*, 2001, **319**, 117; (i) N. W. Alcock, P. Moore and S. Sangha, private communication, 2005; (j) D. Maganas, S. S. Staniland, A. Grigoropoulos, F. White, S. Parsons, N. Robertson, P. Kyritsis and G. Pneumatikakis, *Dalton Trans.*, 2006, 2301; (k) M. C. Aragoni, M. Arca, M. B. Carrea, A. Garau, F. A. Devillanova, F. Isaia, V. Lippolis, G. L. Abbati, F. Demartin, C. Silvestru, S. Demeshko and F. Meyer, *Eur. J. Inorg. Chem.*, 2007, 4607; (l) E. Ferentinos, S. D. Chatziefthimiou, N. Robertson and P. Kyritsis, *Inorg. Chem. Commun.*, 2009, **12**, 615; (m) E. Ferentinos, D. Maganas, C. P. Raptopoulou, A. Terzis, V. Psycharis, N. Robertson and P. Kyritsis, *Dalton Trans.*, 2011, **40**, 169.
- (a) T. S. Khodashova, V. P. Nikolaev, M. A. Porai-Koshits, L. A. Butman, E. I. Tabidze and G. V. Tsintsadze, *Koord. Khim.*, 1986, **12**, 128; (b) W. Bensch and M. Schuster, *Z. Anorg. Allg. Chem.*, 1994, **620**, 1479; (c) W. Bensch and M. Schuster, *Z. Kristallogr.*, 1995, **210**, 68; (d) L. Beyer, R. Richter and O. Seidelmann, *J. Prakt. Chem.*, 1999, **341**, 704; (e) J. D. Crane and M. Whittingham, *Acta Crystallogr., Sect. E: Struct. Rep. Online*, 2004, **60**, m350; (f) Z. Weiqun, Y. Wen, X. Liqun and C. Xianchen, *J. Inorg. Biochem.*, 2005, **99**, 1314; (g) M. F. Emen, H. Arslan, N. Kulcu, U. Florke and N. Duran, *Pol. J. Chem.*, 2005, **79**, 1615; (h) A. Rodenstein, R. Richter and R. Kirmse, *Z. Anorg. Allg. Chem.*, 2007, **633**, 1713; (i) H. Perez, Y. Mascarenhas, A. M. Plutin, R. de S. Correa and J. Duque, *Acta Crystallogr., Sect. E: Struct. Rep. Online*, 2008, **64**, m503; (j) H. Perez, R. S. Correa, A. M. Plutin, B. O'Reilly and J. Duque, *Acta Crystallogr., Sect. E: Struct. Rep. Online*, 2008, **64**, m733; (k) K. Ramasamy, M. A. Malik, P. O'Brien and J. Raftery, *Dalton Trans.*, 2010, **39**, 1460; (l) K. Ramasamy, M. A. Malik, J. Raftery, F. Tuna and P. O'Brien, *Chem. Mater.*, 2010, **22**, 4919; (m) N. Gunasekaran, P. Jerome, S. W. Ng, E. R. T. Tiekink and R. Karvembu, *J. Mol. Catal. A: Chem.*, 2012, **353**, 156.
- For examples: (a) F. D. Sokolov, V. V. Brusko, N. G. Zabiroy and R. A. Cherkasov, *Curr. Org. Chem.*, 2006, **10**, 27; (b) F. D. Sokolov, V. V. Brusko, D. A. Safin, R. A. Cherkasov and N. G. Zabiroy, Coordination diversity of N-phosphorylated amides and ureas towards VIIIIB group cations, in *Transition Metal Chemistry: New Research*, ed. B. Varga and L. Kis, 2008, p. 101 and references therein.
- (a) F. D. Sokolov, D. A. Safin, N. G. Zabiroy, L. N. Yamalieva, D. B. Krivolapov and I. A. Litvinov, *Mendeleev Commun.*, 2004, **14**, 51; (b) D. A. Safin, F. D. Sokolov, N. G. Zabiroy, V. V. Brusko, D. B. Krivolapov, I. A. Litvinov, R. C. Luckay and R. A. Cherkasov, *Polyhedron*, 2006, **25**, 3330; (c) F. D. Sokolov, N. G. Zabiroy, L. N. Yamalieva, V. G. Shtyrlin, R. R. Garipov, V. V. Brusko, A. Yu. Verat, S. V. Baranov, P. Mlynarz, T. Glowiak and H. Kozłowski, *Inorg. Chim. Acta*, 2006, **359**, 2087; (d) D. A. Safin, P. Mlynarz, F. E. Hahn, M. G. Babashkina, F. D. Sokolov, N. G. Zabiroy, J. Galezowska and H. Kozłowski, *Z. Anorg. Allg. Chem.*, 2007, **633**, 1472; (e) D. A. Safin, P. Mlynarz, F. D. Sokolov, M. Kubiak, F. E. Hahn, M. G. Babashkina, N. G. Zabiroy, J. Galezowska and H. Kozłowski, *Z. Anorg. Allg. Chem.*, 2007, **633**, 2089; (f) D. A. Safin, M. Bolte and M. G. Babashkina, *Transition Met. Chem.*, 2009, **34**, 43; (g) D. A. Safin, M. Bolte, M. G. Babashkina and A. Klein, *Russ. J. Gen. Chem.*, 2010, **80**, 1263; (h) D. A. Safin, M. G. Babashkina, M. Bolte, L. Szyrwił, A. Klein and H. Kozłowski, *Phosphorus, Sulfur Silicon Relat. Elem.*, 2010, **185**, 1739; (i) M. G. Babashkina, D. A. Safin, M. Bolte and A. Klein, *Heteroat. Chem.*, 2010, **21**, 486; (j) M. G. Babashkina, D. A. Safin, M. Bolte and A. Klein, *Acta Chim. Slov.*, 2010, **57**, 475; (k) M. G. Babashkina, D. A. Safin, A. Railliet, M. Bolte, A. Brzuszkiewicz, H. Kozłowski and Y. Garcia, *New J. Chem.*, 2012, **36**, 2642.
- N. G. Zabiroy, V. V. Brusko, A.Y. Verat, D. B. Krivolapov, I. A. Litvinov and R. A. Cherkasov, *Polyhedron*, 2004, **23**, 2243.
- (a) H. Hahn and W. Kligen, *Naturwissenschaften*, 1965, **52**, 494; (b) W. Kligen, R. Ott and H. Hahn, *Z. Anorg. Allg. Chem.*, 1973, **396**, 271.

- 7 (a) D. A. Cleary and A. H. Francis, *J. Phys. Chem.*, 1988, **92**, 2415; (b) Z. Mielke, G. D. Brabson and L. Andrews, *J. Phys. Chem.*, 1991, **95**, 75.
- 8 M. Sarkar, R. Clérac, C. Mathonière, N. G. R. Hearn, V. Bertolasi and D. Ray, *Eur. J. Inorg. Chem.*, 2009, 4675.
- 9 M. Idesikova, L. Dlhán, J. Moncol, J. Titis and R. Boca, *Polyhedron*, 2012, **36**, 79.
- 10 *CrysAlisPro*, Agilent Technologies, Version 1.171.36.21, 2012.
- 11 G. M. Sheldrick, *Acta Crystallogr., Sect. A: Found. Crystallogr.*, 2008, **64**, 112.
- 12 I. J. Bruno, J. C. Cole, P. R. Edgington, M. Kessler, C. F. Macrae, P. McCabe, J. Pearson and R. Taylor, *Acta Crystallogr., Sect. B: Struct. Sci.*, 2002, **58**, 389.